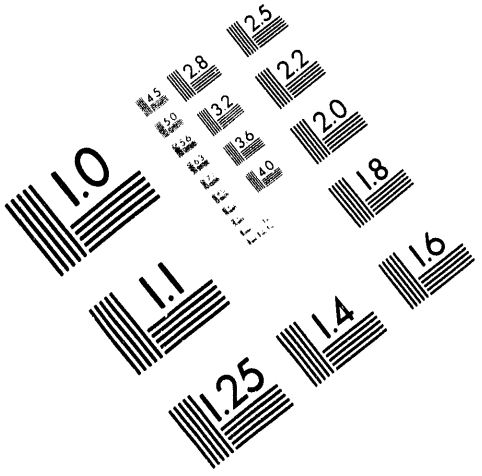

Association for Information and Image Management

1100 Wayne Avenue, Suite 1100
Silver Spring, Maryland 20910

301/587-8202

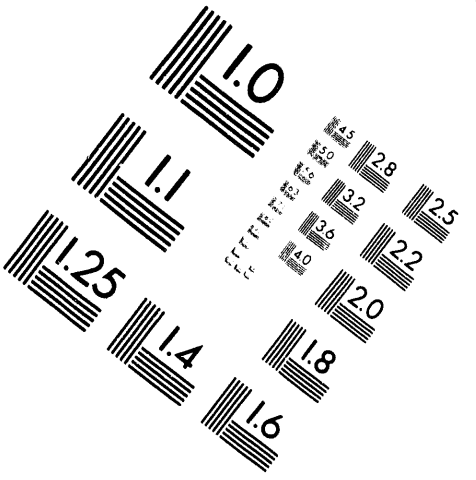

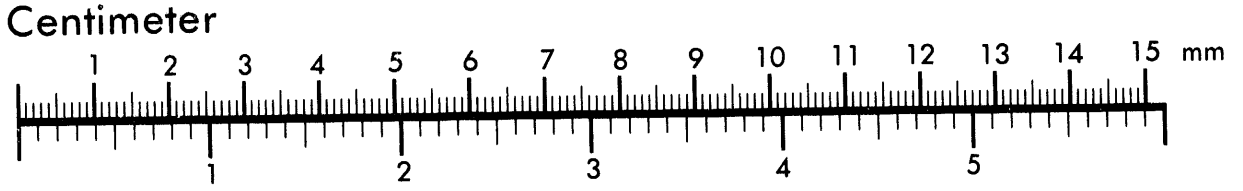

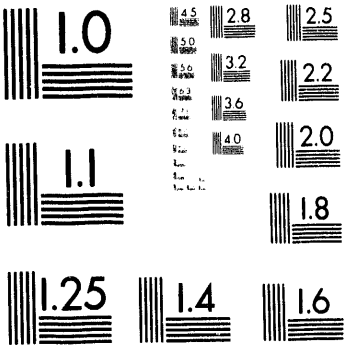

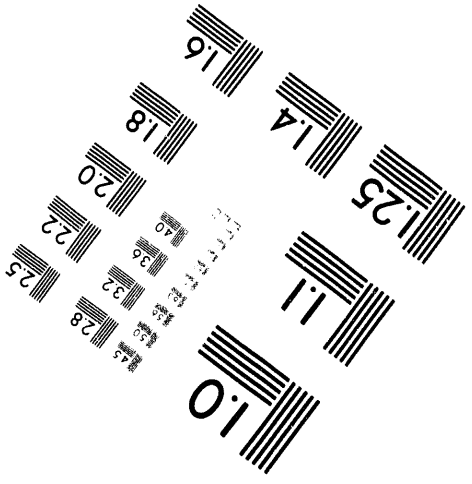

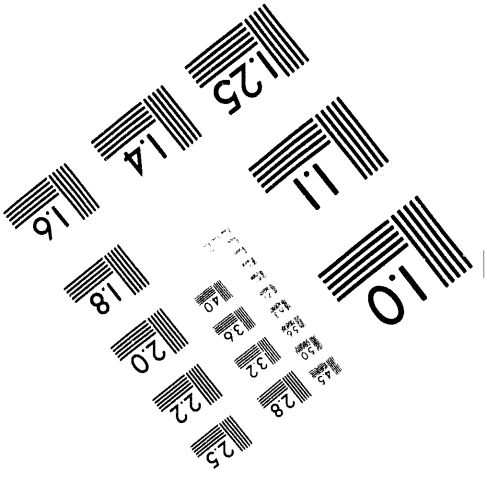

1 of 1

MODELING INFILTRATION INTO A TUFF MATRIX FROM A SATURATED VERTICAL FRACTURE

Clifford K. Ho

Sandia National Laboratories
P.O. Box 5800, Org. 6115
Albuquerque, NM 87185-1324
(505) 848-0712

ABSTRACT

Saturation profiles resulting from TOUGH2 numerical simulations of water infiltration into a tuff matrix from a saturated vertical fracture have been compared to experimental results. The purpose was to determine the sensitivity of the infiltration on local heterogeneities and different representations of two-phase characteristic curves used by the model. Findings indicate that the use of simplified (linearized) capillary pressure curves with rigorous (van Genuchten) relative permeability curves resulted in a more computationally efficient solution without a loss in accuracy. However, linearized forms of the relative permeability functions produced poor results, regardless of the form of the capillary pressure function. In addition, numerical simulations revealed that the presence of local heterogeneities in the tuff caused non-uniform saturation distributions and wetting fronts in the matrix.

I. INTRODUCTION

Predictive models of hydrologic transport in the subsurface are used in many disciplines including environmental remediation and nuclear waste management. An area of growing interest in these fields lies in the unsaturated zone, where both spilled contaminants and potential nuclear waste repositories can reside. For example, the evaluation of Yucca Mountain as a potential high-level radioactive waste repository relies on predictive hydrologic models in unsaturated tuff surrounding the proposed site. Since the transport of contaminants and radionuclides can depend

strongly on hydrologic behavior in these unsaturated regions, models typically use two-phase characteristic curves which govern hydrologic flow in the unsaturated zone. Capillary pressures and relative permeabilities are often expressed as non-linear functions of liquid saturation, and these are used in the models to determine liquid and gas phase mobilities. However, due to the highly non-linear nature of these functions, computational efficiency can be greatly reduced in the numerical codes. For example, at low liquid saturations the capillary pressures used in the models are often discontinuous or extremely large, forcing numerous iterations and reductions in the time-steps used by the numerical code. In addition, low liquid saturations in low permeability media give rise to extremely high capillary pressures that can imply negative absolute liquid-phase pressures. The validity of using these extreme values for calculating liquid mobilities has been questioned by previous investigators[1].

The objective of this study is to identify simplified two-phase characteristic curves that relax the computational burden while maintaining the physical integrity of the model. Infiltration into an unsaturated tuff matrix from a saturated vertical fracture is considered for the analysis. Numerical results are compared to an experiment performed by Foltz et al.[2] in which saturation fields were recorded during two-dimensional imbibition into a tuff slab taken from the Nevada Test Site. Both rigorous and simplified forms of the two-phase characteristic curves are used in the numerical model to identify appropriate forms of the curves that accurately represent the physical system while providing computationally efficient solutions. In addition, the effects of local heterogeneities in the tuff matrix are investigated by comparing saturation distributions resulting from numerical simulations using both homogeneous and heterogeneous permeability fields.

II. INVESTIGATIVE APPROACH

In this section, necessary background is provided for the analysis presented in this report. First, two-phase characteristic curves are described, and the different forms used in this study are presented and discussed. Then, a brief description of the two-dimensional imbibition experiment

presented in Foltz et al.[2] is given. Finally, the numerical approach used in the simulation of the experiment is presented.

A. Two-Phase Characteristic Curves

In order to characterize hydrologic behavior in unsaturated regions, capillary pressure and relative permeability curves must be measured for the media of interest. In the water-air system considered in this study, the capillary pressure functions give a measure of the tendency of the porous medium to imbibe water, the wetting fluid. The relative permeability functions give a measure of the impedance of flow of one fluid phase due to the presence of another fluid phase. Both capillary pressure and relative permeability curves can be generated using various experimental methods,[3] and curve-fitting expressions approximating these data such as the Brooks and Corey[4] and van Genuchten[5] functions can be used in the models.

Due to the lack of data characterizing the tuff used in the experiments performed by Foltz et al.,[2] capillary pressure and relative permeability functions (and fitting parameters) used by Pruess[6] to model flow in a tuffaceous rock are used in this study as well. The parameters were taken from Hayden et al.,[7] where hydrologic modeling of the Topopah Spring Unit of Yucca Mountain was performed. The van Genuchten functions used to characterize the capillary pressures, P_c, and liquid-phase relative permeabilities, $k_{r,w}$, as a function of liquid saturation, S, in the tuff are given as follows:

$$P_c = \frac{1}{\alpha}\left(S_e^{-1/m} - 1\right)^{1-m} \tag{1}$$

$$k_{r,w} = S_e^{0.5}\left(1 - \left(1 - S_e^{1/m}\right)^m\right)^2 \tag{2}$$

where $$S_e = \frac{S - S_r}{1 - S_r}$$

and m=0.45, $\alpha = 7.178\text{x}10^{-7}$, and $S_r = 0.0$

In the above equations, α and m are curve fitting parameters, S_e is an effective saturation, and S_r is the residual liquid saturation. Equations (1) and (2) are plotted in Figures 1 and 2 (the plotted values of the capillary pressures are negative to symbolize capillary suction). Note the highly non-linear dependence of both the capillary pressure and relative permeability on the liquid saturation. As stated earlier, computational performance can be hindered due to the non-linear nature of these curves. As a result, alternative linearized functions of the capillary pressures and relative permeabilities were also used in the numerical simulations for comparison. These linearized functions are also plotted in Figures 1 and 2 and are given as follows:

$$P_c = -6\text{x}10^6 + 6\text{x}10^6 S \tag{3}$$

$$k_{r,w} = S \tag{4}$$

Numerous simplified curves could have been chosen to represent the non-linear functions given in Equations (1) and (2), but the primary objectives of this study were to minimize the non-linearity of the curves and to eliminate any discontinuities over the entire liquid saturation domain ($0 \leq S \leq 1$). For example, a linear representation of the relative permeability function could have been chosen such that the liquid relative permeability decreased to zero at a liquid saturation of 0.7 instead of 0, but a slope discontinuity would exist at that value, potentially creating complications in convergence in the numerical code. Thus, the linear relative permeability and capillary pressure curves given in Equations (3) and (4) were chosen to span the entire range of liquid saturations ($0 \leq S \leq 1$). In addition, the slope of the linear capillary pressure curve was chosen to best approximate the given capillary pressures in Equation (1).

Figure 2 shows a large discrepancy between the relative permeabilities as given by the van Genuchten and the linearized functions for all values of liquid saturation. It is apparent that the use of the linearized relative permeability function should yield more diffusive or 'smeared' wetting fronts during infiltration into a porous matrix, while the van Genuchten function should produce a sharper wetting front. Figure 1 shows that the linearized form of the capillary pressure function

deviates significantly from the van Genuchten function only at low liquid saturations. Because the van Genuchten relative permeabilities are essentially zero at these low liquid saturations, the use of the linearized form of the capillary pressure function with the van Genuchten relative permeability function are expected to produce results that are similar to those using both van Genuchten capillary pressure and relative permeability functions. Computational savings are expected to occur in this case since the highly non-linear capillary pressures are avoided at the lower liquid saturations.

B. Experimental Background

In the experiments performed by Foltz et al.[2], two slabs of tuff (each 14.0 cm high x 10.2 cm wide x 2.5 cm thick) were cut from a block of partially welded Timber Mountain Tuff obtained from the Nevada Test Site. An approximate 100 micron gap (slot fracture) was maintained between the vertical edges of the two slabs, which were held in place with an aluminum frame. A potassium iodide solution (an image contrast enhancing agent) was introduced at a constant rate of 1.7 ml/min at the top of the gap. X-ray adsorption imaging[8] was then used to capture transient liquid saturation fields in the initially dry slabs of tuff. Images of the saturation fields (512x512 pixels cropped down to 260x280 pixels) were obtained from x-ray exposures lasting 100 seconds. Figure 3 shows a sketch of the tuff slabs, the boundary conditions, and inclusions (possibly pumice) that were visible in the tuff slabs. The visible inclusions acted as barriers to flow and are discussed in detail later. At the fracture outlet slight aspiration was applied to simulate a continuous fracture. However, experimental difficulties were encountered resulting in inadvertent ponding of water at the outlet.

Figures 4(a)-(d) show the saturation fields in the tuff slabs at 123, 957, 1890, and 3903 seconds following initiation of the experiment as reported by Foltz et al.[2] Black represents completely dry conditions and white represents completely saturated conditions (the white vertical strip in the center is the location of the fracture). Note that the images were cropped by the aluminum frame so that the dimensions of each tuff slab in the images are slightly reduced (14.0

cm high x 8.5 cm wide). Figure 4 shows that a non-uniform wetting front propagated into the tuff slabs. The cause of this non-uniformity was suspected to be a combination of the local heterogeneities in the tuff matrix and the ponded boundary condition described earlier. Figure 5 provides saturation data along a horizontal transect located 6.5 cm below the top edge of the right-hand tuff slab (x=0 corresponds to the location of the vertical fracture). Note that Figure 5 shows that the wetting fronts are very sharp for all recorded times. Both Figures 4 and 5 are used in comparing liquid saturation distributions with the numerical simulations.

C. Numerical Approach

Numerical simulations of the experimental system were run using TOUGH2[9]. TOUGH2 (Transport Of Unsaturated Groundwater and Heat) is a numerical code developed by Pruess[9] to model the coupled transport of air, water, vapor, and heat in porous media. The mathematical formulation used in the code is presented in Pruess[9], so only the grid formulation and physical models are presented here. Two simulation studies were performed using TOUGH2 to determine the sensitivity of the infiltration process into a tuff matrix to different representations of two-phase characteristic curves and local heterogeneities. In both studies, saturation profiles were generated by the numerical models at times corresponding to those recorded during the experiment to facilitate comparison.

In the first study, a homogeneous TOUGH2 grid shown in Figure 6 was used to model the infiltration experiment performed by Foltz et al.[2] (only the right-hand tuff slab was modeled for simplicity). A homogeneous grid infers that the properties of all the elements in the grid such as bulk permeability and porosity are uniform. This homogeneous case was used to determine the sensitivity of the simulation to different combinations of two-phase characteristic curves. Four simulations were run using different combinations of the characteristic curves shown in Figures 1 and 2. A saturated boundary on the left side of the grid was used to simulate the saturated vertical fracture (in the experiments water propagated rapidly through the vertical gap, so a saturated vertical boundary was assumed in the simulations). The right boundary was maintained at

atmospheric pressure and zero saturation, and no flow conditions were imposed on all other boundaries. The tuff elements shown in Figure 6 were initially dry, and at t=0 water was allowed to imbibe into the matrix from the saturated elements along the left edge of the matrix. Table 1 contains the properties of the tuff elements that were used in the model. These parameters (except for the experimentally measured porosity) were taken from Pruess[6] who used values compiled by Hayden et al.[7] during hydrologic modeling of the Topopah Spring Unit of Yucca Mountain.

In the second study, heterogeneous hydraulic properties were used to determine the effects of local heterogeneities and the ponding of water at the fracture outlet on the infiltration experiment. Figure 7 shows the permeability field that was used in these simulations. The grid was identical to the homogeneous grid except for two modifications. First, a low permeability element was added along the left edge of the TOUGH2 grid to simulate a visible inclusion in the actual tuff matrix. The visible heterogeneity acted as a barrier to flow, but the actual properties of the inclusion were unknown. Therefore, the heterogeneous element was given a permeability that was two orders of magnitude lower than the rest of the matrix (the actual inclusion may have had a larger porosity than the rest of the matrix, acting as a capillary barrier to flow; in either case the intention here was to create an element which simply acted as a flow barrier). Second, two saturated elements were added to the bottom of the grid to simulate the ponding of water as observed during the experiment. These modifications were expected to provide full-field saturation distributions which resembled the experimental saturation fields more closely than the homogeneous results. The properties of the tuff elements used in this study are shown in Table 1.

III. RESULTS AND DISCUSSION

A. Homogeneous Simulations

Four homogeneous simulations were performed using different combinations of characteristic curves shown in Figures 1 and 2. Figures 8(a)-(d) show the two-dimensional full-field saturation fields in the right-hand tuff matrix at 3903 seconds of infiltration for each combination. Recall that

only the right-hand tuff slab was modeled for simplicity. A comparison of these figures with the experimentally observed saturation fields shown in Figure 4 reveals that the use of linear relative permeability curves in the numerical model (Figures 8(a) and 8(b)) results in wetting fronts that are too diffuse. The use of non-linear relative permeability functions (Figures 8(c) and 8(d)) results in sharper wetting fronts that more closely resemble the experimental observations. However, the simulated wetting fronts are all vertically uniform, whereas the experimentally observed wetting fronts are vertically non-uniform. The discrepancy is attributed to local heterogeneities and boundary conditions not included in this set of simulations. The heterogeneous simulations will address this issue further.

Saturation profiles were numerically generated at times corresponding to the experiment along a horizontal transect of the tuff matrix 6.5 cm from the top. Figures 9(a)-(d) give the saturation profiles for the different combinations of characteristic curves. In Figures 9(a) and 9(b) it is apparent that the use of linearized forms of the relative permeability functions results in smeared saturation fronts, regardless of the form of the capillary pressure function. On the other hand, the use of non-linear van Genuchten relative permeability functions corresponds more closely to the observed experimental profiles as shown in Figures 9(c) and 9(d). In these two cases, steeper saturation fronts are observed, and the results of using a linearized capillary pressure function (Figure 9(c)) are very similar to the results of the simulation using the non-linear van Genuchten capillary pressure function (Figure 9(d)). Thus, despite the different capillary pressure representations, the resulting saturation distributions were very similar when non-linear relative permeability functions were used. This was expected since the capillary pressures differed only below a liquid saturation of 0.4 as shown in Figure 1, and below this value the van Genuchten relative permeabilities were very close to zero as shown in Figure 2. Therefore, the liquid mobility at this saturation was essentially zero, and discrepancies between the linear and non-linear capillary pressure curves at low liquid saturations did not have significant impacts on the results. In addition, the use of the linearized form of the capillary pressure function resulted in runs with computation times that were over 40% faster than those using the non-linear function.

B. Heterogeneous Simulations

In this section we attempt to explain the non-uniform wetting front observed experimentally as shown in Figure 4. The only differences between this simulation and the homogeneous simulations are the addition of a low permeability region in the tuff matrix and additional saturated boundary elements along the bottom left edge of the grid as shown in Figure 5. Since it was learned from the homogeneous simulations that the use of linear relative permeability functions resulted in poor results, only the non-linear van Genuchten relative permeability function was used in the heterogeneous simulation. Also, since the use of the linear capillary pressure function provided similar results as the non-linear van Genuchten capillary pressure function in the homogeneous simulations with a savings in computational time, only the linear capillary pressure function was used.

Figures 10(a)-(d) show the two-dimensional full-field saturation fields resulting from the numerical simulation at 123, 957, 1890, and 3903 seconds of infiltration from the saturated boundary along the left edge. The inclusion has a notable effect of retarding the infiltration in that region as shown by both the numerical simulations (Figure 10) and the experimental saturation profiles (Figure 4). Note that the region near the inclusion in the experiment remained at a low liquid saturation even after the wetting front had passed as shown in Figure 4(d). However, the numerically simulated low permeability inclusion becomes fully saturated as shown in Figure 10(d). This indicates that the inclusion was most likely a high porosity region which acted as a capillary barrier, successfully preventing flow into the inclusion. There is also a significant change in the saturation distribution near the bottom as a result of the additional saturated elements. Comparison of these saturation fields with those of the experiment in Figures 4(a)–(d) reveal a similar wetting front behavior. The rather simple modifications that included one low permeability element and two additional saturated boundary elements were sufficient to yield more realistic saturation profiles than those resulting from the homogeneous simulation.

IV. CONCLUSIONS

The use of appropriate two-phase characteristic curves in hydrologic models of unsaturated flow in tuff has been investigated. The need for alternative forms of the characteristic curves is sometimes necessary for feasible, computationally efficient models of unsaturated flow problems such as the evaluation of Yucca Mountain as a potential high-level radioactive waste repository. Infiltration into a tuff matrix has been simulated numerically and experimentally, and comparisons of saturation distributions have been made between the numerical and experimental results using both linear and non-linear (van Genuchten) forms of the two-phase characteristic curves. While linearized forms of the relative permeability functions produced poor results, the use of linearized forms of the capillary pressure function yielded reasonable solutions when non-linear relative permeability functions were used. The use of linearized capillary pressure functions also increased computational speed by over 40%. This implies that the use of simplified capillary pressure curves may provide a reasonable alternative to highly non-linear curves if increased computational efficiency is desired while maintaining the integrity of the physical solution. Recall, however, that these findings are based on the analysis of just one experiment and one simplified form of the two-phase characteristic curves. Future studies using other forms and combinations of simplified two-phase characteristic curves need to be investigated with additional experiments to confirm this assertion.

Finally, this study revealed that local property variations in the tuff matrix and boundary conditions significantly altered the uniform imbibition of liquid into the tuff matrix at the scale under investigation. The effects of such heterogeneities are expected to be dependent on the relative size and severity of the heterogeneities relative to the matrix. Therefore, rigorous simulations of hydrologic behavior in heterogeneous environments need to be performed in conjunction with homogeneous simulations to determine the relative effects of heterogeneities at the scale under investigation.

ACKNOWLEDGMENTS

This work was performed for the U.S. Department of Energy, Yucca Mountain Site Characterization Project, under contract DE-AC04-94AL85000. The author would like to acknowledge Sue Foltz for obtaining the experimental data for this report. Communication with Steve Webb, Bob Glass, Vince Tidwell, and Mike Nicholl during this study is also appreciated.

NOMENCLATURE

CP	Capillary pressure
k	Bulk permeability
$k_{r,w}$	Relative permeability of the wetting fluid
m	Curve-fitting parameter in the van Genuchten functions
P_c	Capillary pressure
RP	Relative permeability
S	Liquid saturation
S_e	Effective saturation used in the van Genuchten functions
S_r	Residual liquid saturation
t	Time
α	Curve-fitting parameter in the van Genuchten functions
ϕ	Total porosity
ρ	Density

REFERENCES

1. Gray, W. G. and S. M Hassanizadeh, Paradoxes and Realities in Unsaturated Flow Theory, *Water Resources Research*, Vol. 27, No. 8, pp. 1847-1854, 1991.

2. Foltz, S. D., V. C. Tidwell, R. J. Glass, and S. R. Sobolik, Investigation of Fracture-Matrix Interaction: Preliminary Experiments in a Simple System, Proc. of Fourth Int. Conf. of High Level Rad. Waste Management, Las Vegas, NV, pp. 328-335, 1993.

3. Bear, J., *Dynamics of Fluids in Porous Media*, Dover Publications, Inc., New York, 1972.

4. Brooks, R.H., and A.T. Corey, Hydraulic Properties of Porous Media, Hydrology Papers, No. 3, Colorado State University, March 1964.

5. van Genuchten, M. Th., A Closed-Form Equation for Predicting the Hydraulic Conductivity of Unsaturated Soils, *Soil Sci. Soc. Am. J.*, Vol. 44, pp. 892-898, 1980.

6. Pruess, K., TOUGH User's Guide, Lawrence Berkeley Laboratory, Berkeley, CA, SAND86-7104, LBL-20700, 1987.

7. Hayden, N.K., J.K. Johnstone, and R.R. Peters, Parameters and Material Properties for Hydrologic Modeling of the Topopah Spring Unit, Memo to Distribution, Sandia National Laboratories, September 27, 1983.

8. Tidwell, V.C. and R.J. Glass, X-ray and Visible Light Transmission as Two-Dimensional, Full-Field Moisture Sensing Techniques: A Preliminary Comparison, Proc. of 3rd Int. Conf. of High Level Rad. Waste Management, Las Vegas, NV, pp. 1099-1110.

9. Pruess, K., TOUGH2—A General-Purpose Numerical Simulator for Multiphase Fluid and Heat Flow, LBL-29400, Lawrence Berkeley Laboratory, Berkeley, CA, 1991.

Table 1. Element properties used in TOUGH2 grid (Pruess[6]).

Tuff Property	
density, ρ (kg/m^3)	2550
porosity, ϕ (m^3 pore/m^3 total)	0.27†
permeability, k (m^2)	3.3×10^{-17}

† measured in Foltz et al.[2]

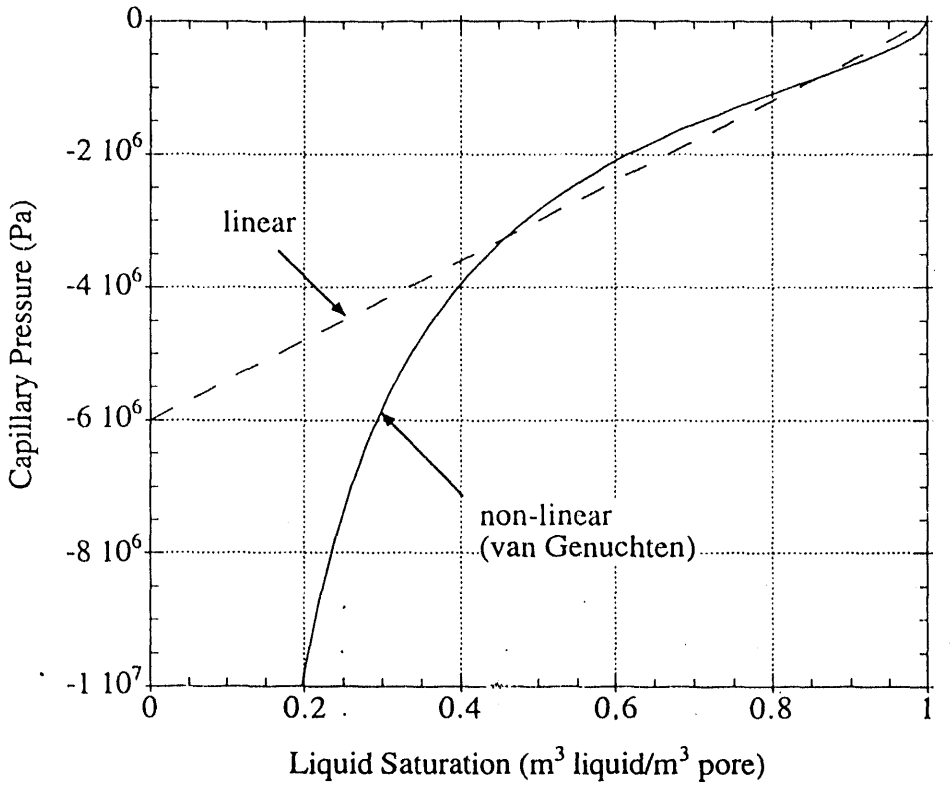

Figure 1. Linear (dashed) and non-linear van Genuchten (solid) capillary pressure curves used in the TOUGH2 simulations.

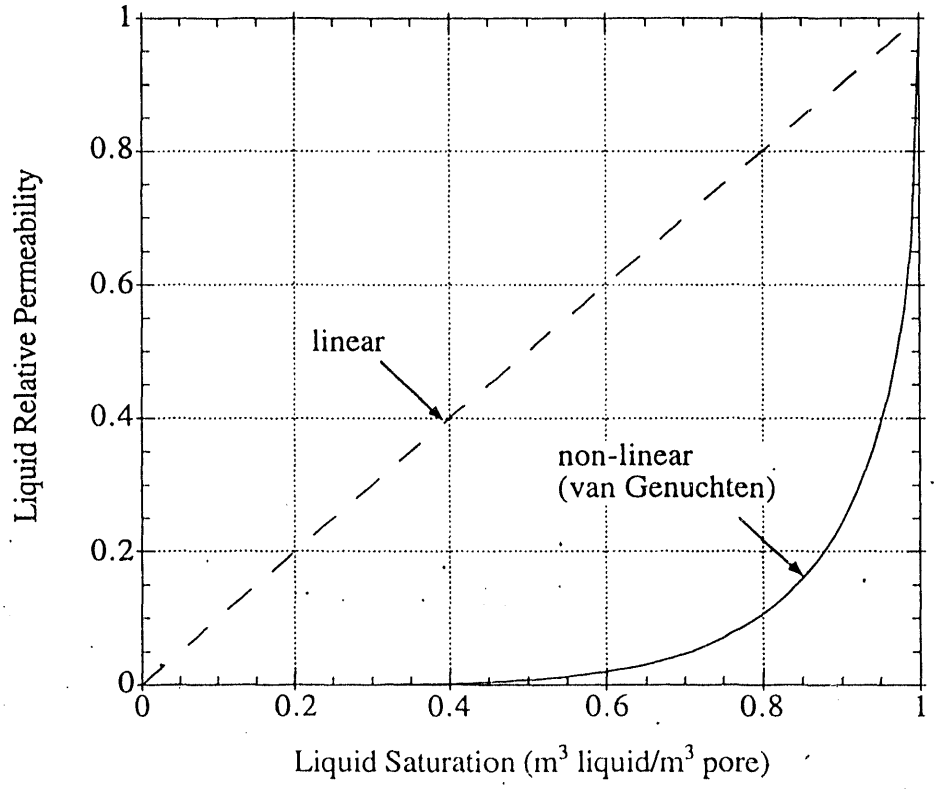

Figure 2. Linear (dashed) and non-linear van Genuchten (solid) liquid relative permeability functions used in the TOUGH2 simulations.

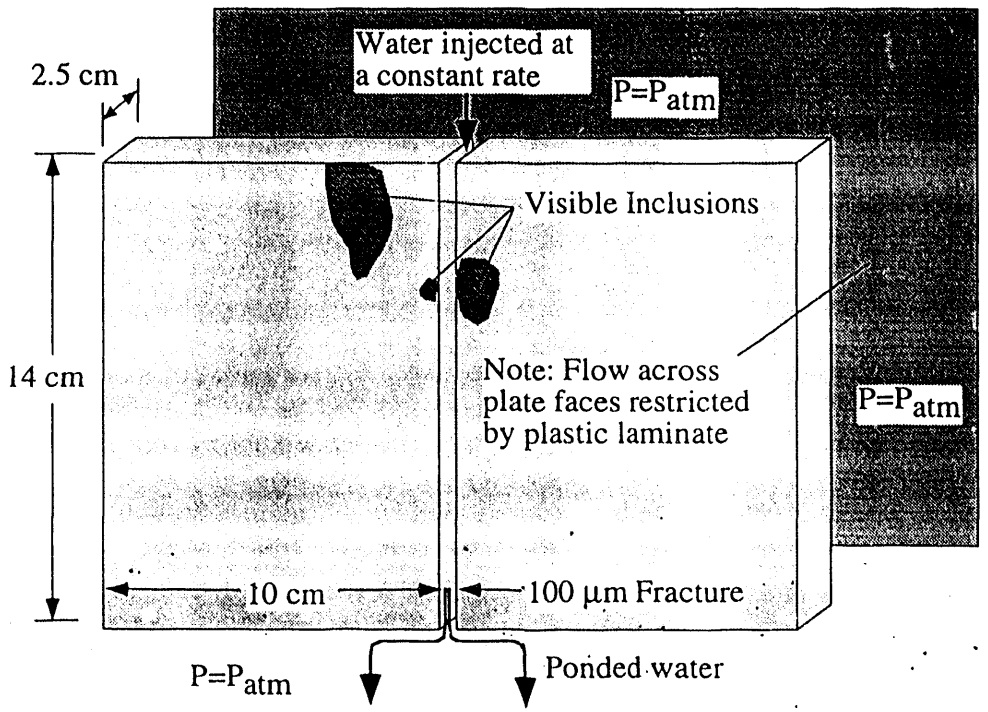

Figure 3. Schematic of the tuff plates and boundary conditions in the fracture-matrix experiment performed by Foltz et al.[2].

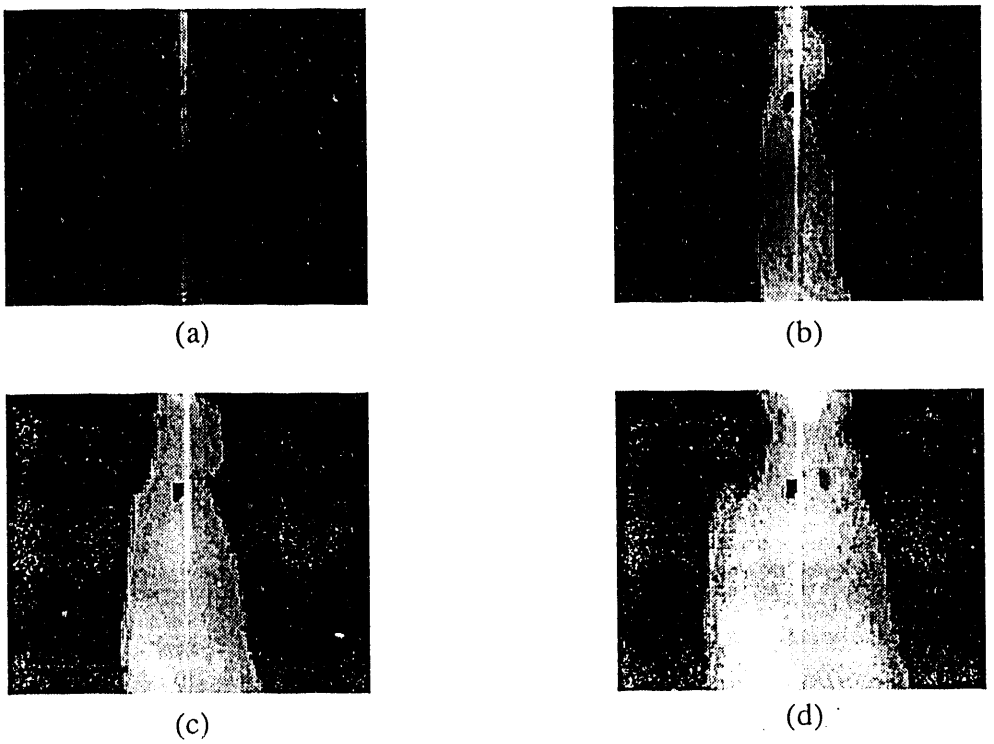

Figure 4. Observed saturation profiles in the tuff plates at a) 123 b) 957 c) 1890 and d) 3903 seconds following injection of water at the top of the vertical fracture. Black corresponds to completely dry and white corresponds to completely saturated. The images were cropped such that the dimensions of each plate are approximately 14 cm high x 8.5 cm wide (Foltz et al.[2]).

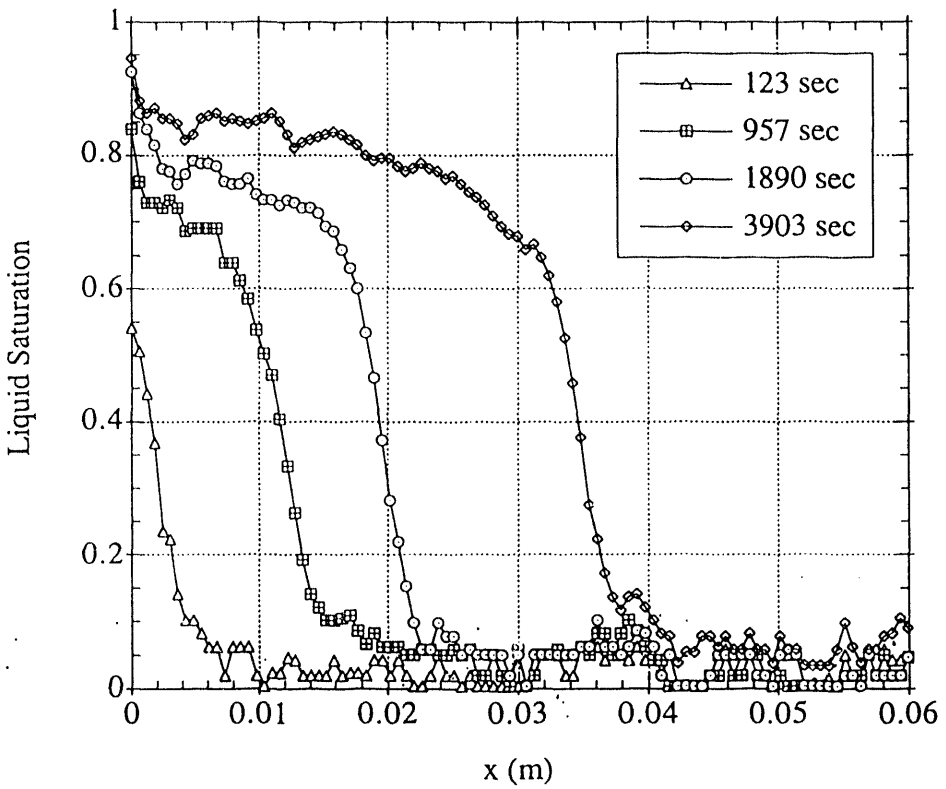

Figure 5. Experimental saturation distributions from Foltz et al.[2] in the right-hand tuff plate along a horizontal transect 6.5 cm from the top of the plate (x=0 corresponds to the fracture location).

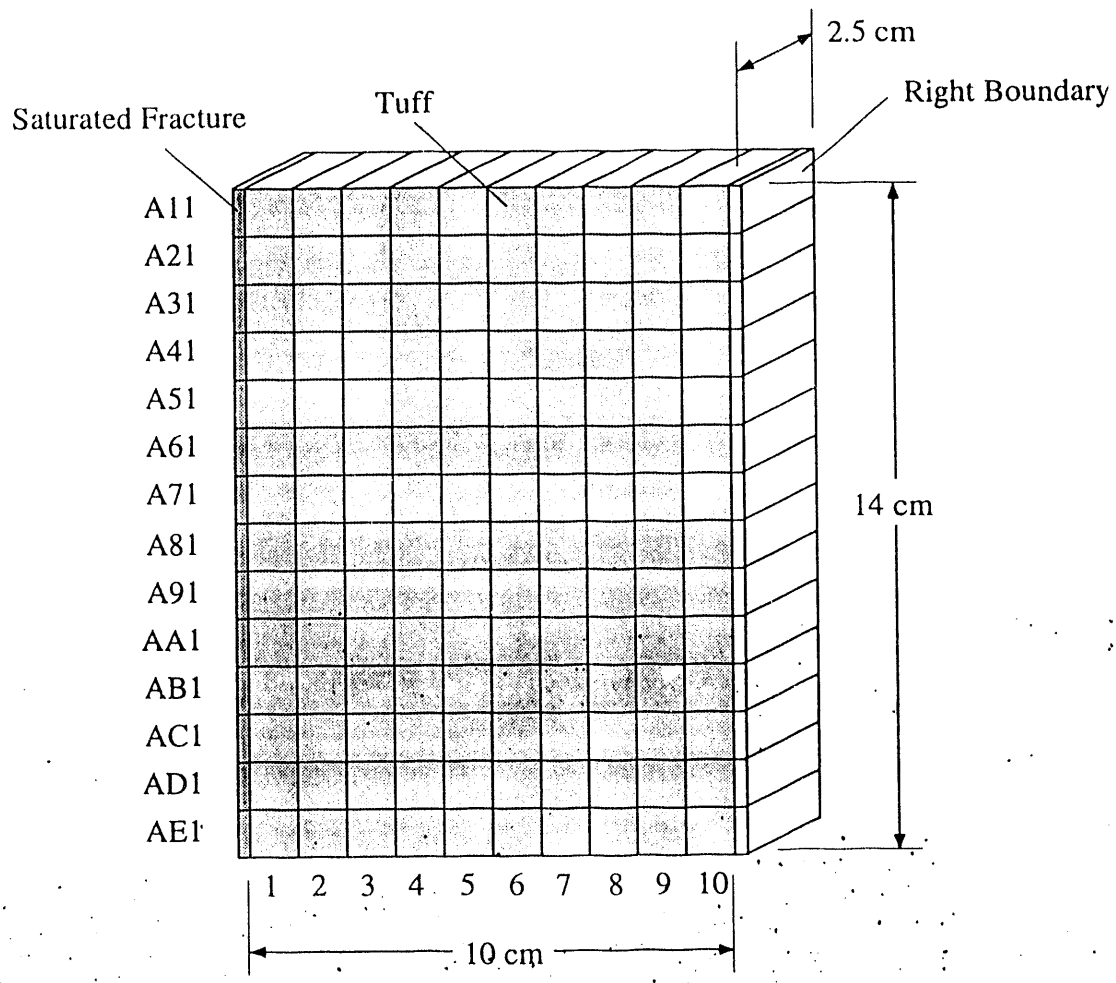

Figure.6. Homogeneous TOUGH2 model used in simulations of water infiltration into a tuff matrix from a saturated vertical fracture.

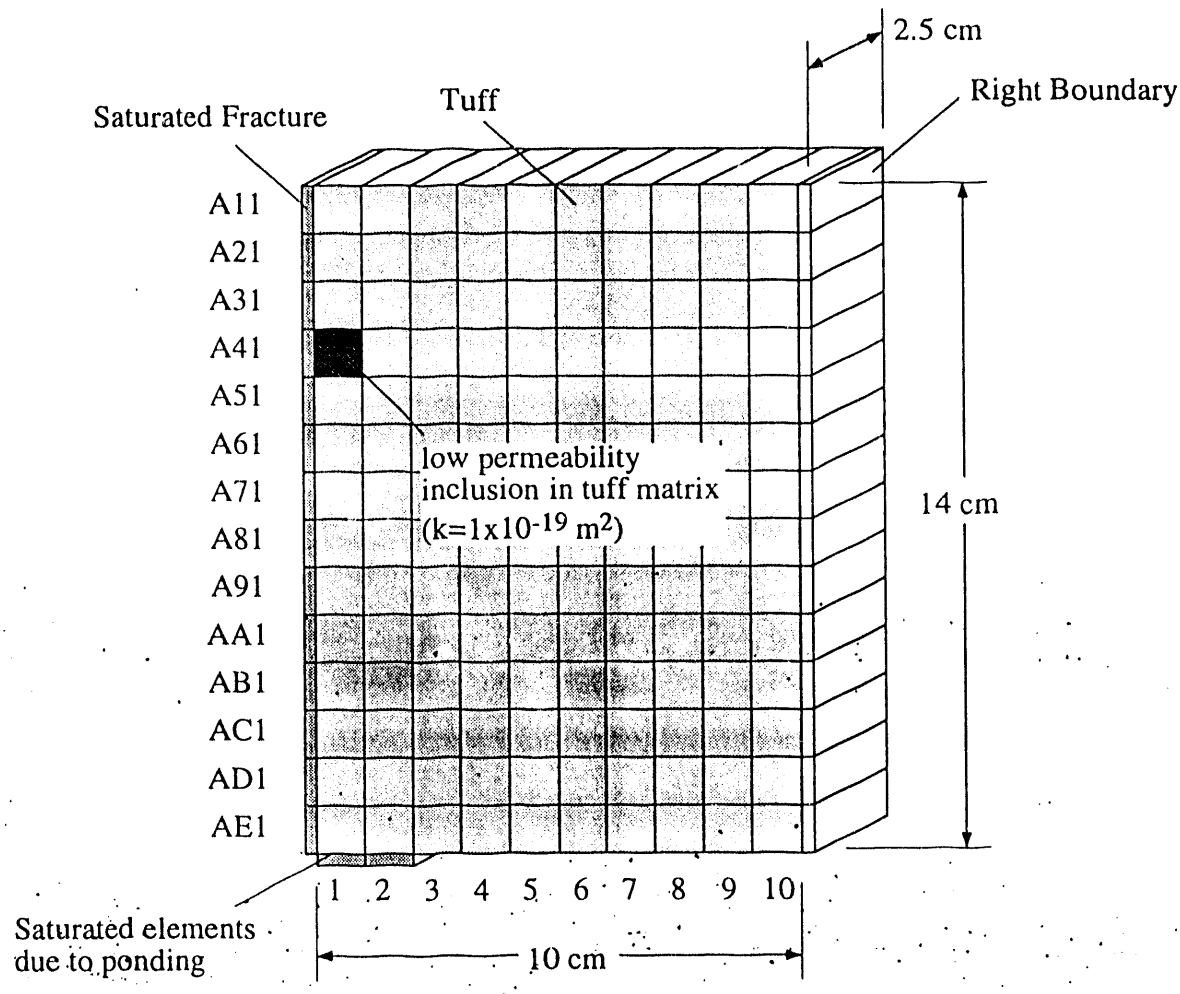

Figure 7. Heterogeneous TOUGH2 grid used in simulations of water infiltration into a tuff matrix from a saturated vertical fracture with ponded water along the bottom. Note: the permeability assigned to the inclusion is only an approximation.

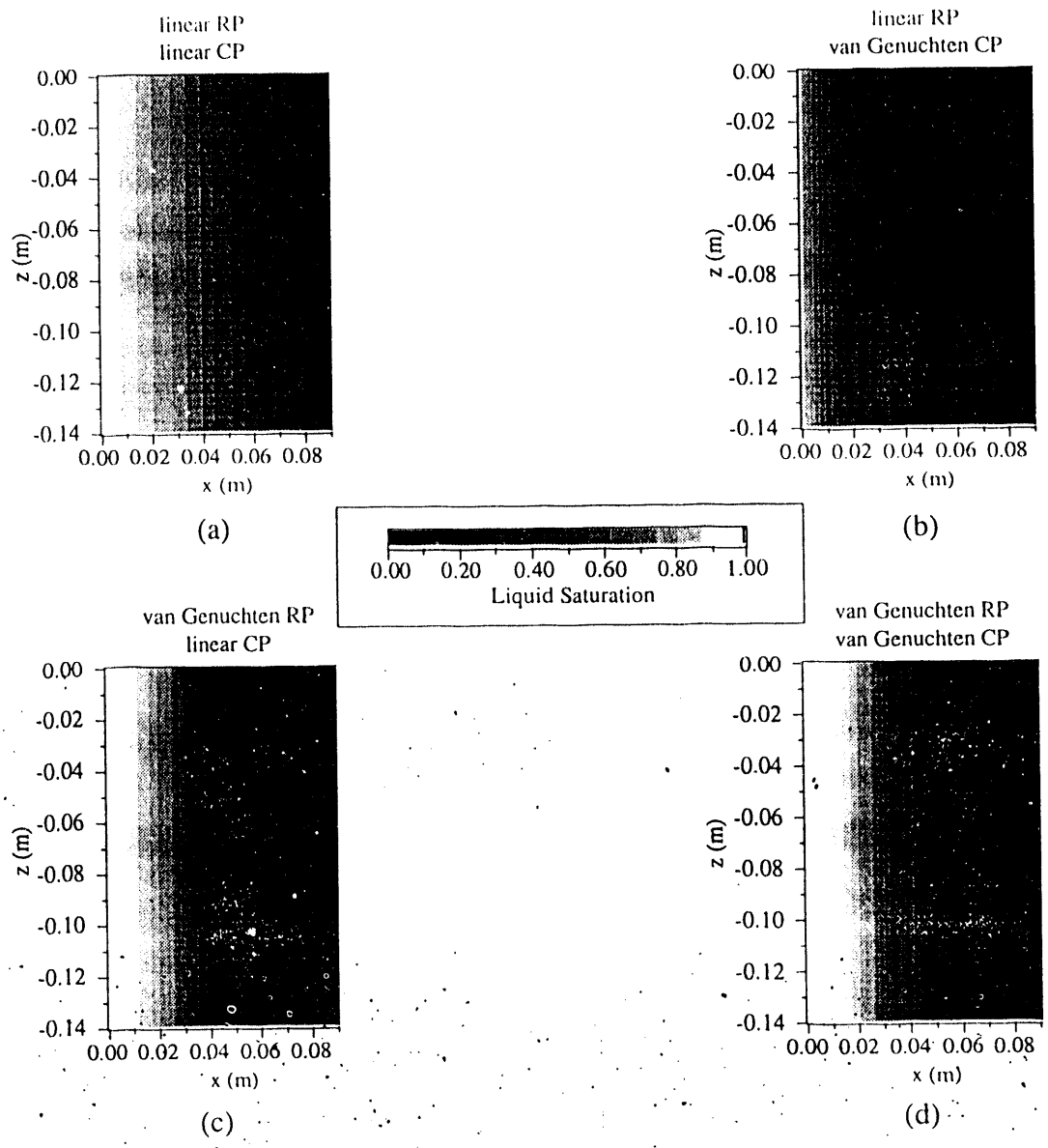

Figure 8. Numerical simulations of liquid saturations in the right-hand homogeneous tuff matrix at 3903 seconds using different combinations of relative permeability (RP) and capillary pressure (CP) functions: a) linear RP, linear CP b) linear RP, van Genuchten CP c) van Genuchten RP, linear CP, and d) van Genuchten RP, van Genuchten CP.

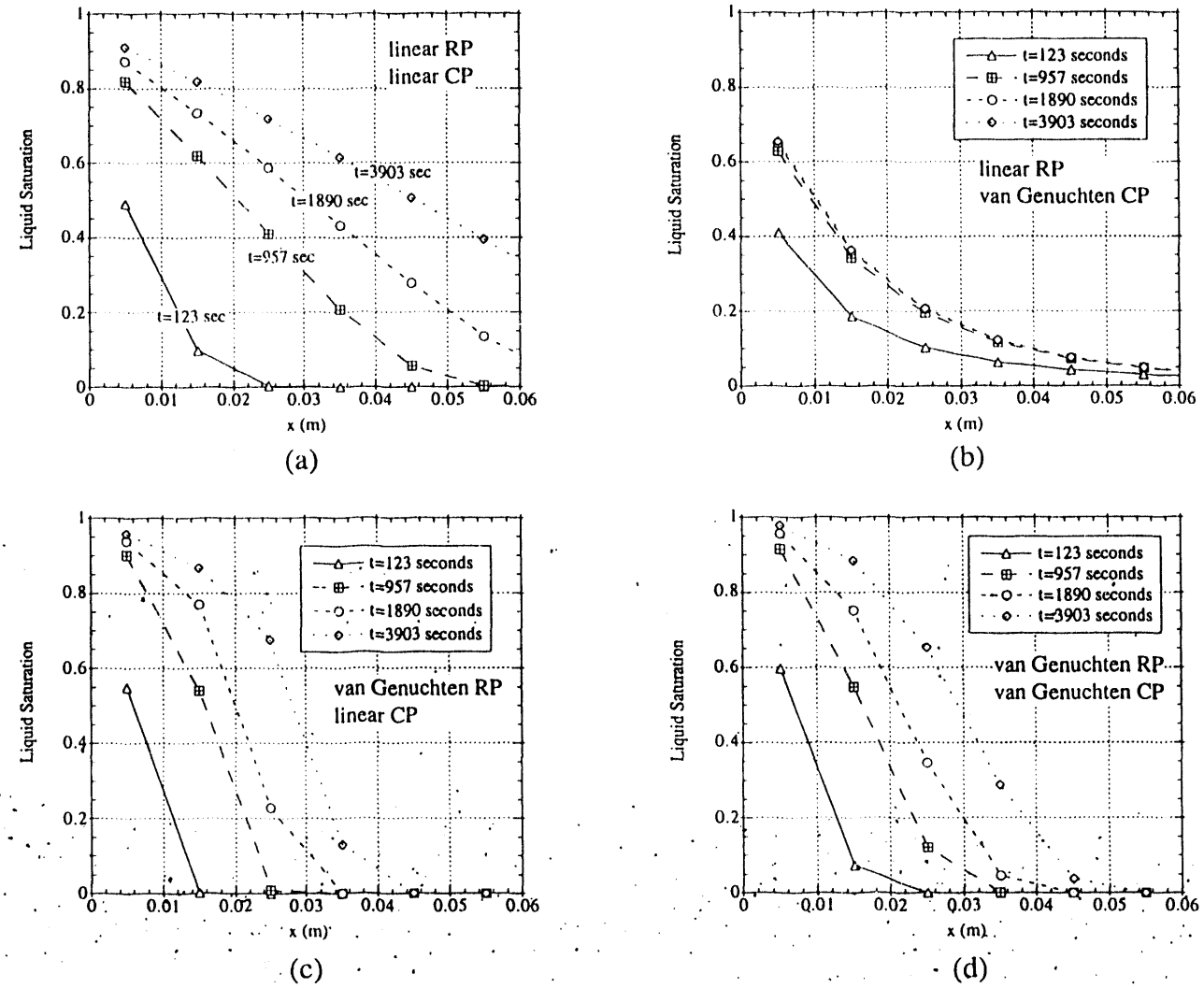

Figure 9. Numerical saturation distributions along a transect 6.5 cm from the top of the right-hand tuff matrix using different combinations of relative permeability (RP) and capillary pressure (CP) functions: a) linear RP, linear CP, b) linear RP, van Genuchten CP c) van Genuchten RP, linear CP and d) van Genuchten RP, van Genuchten CP.

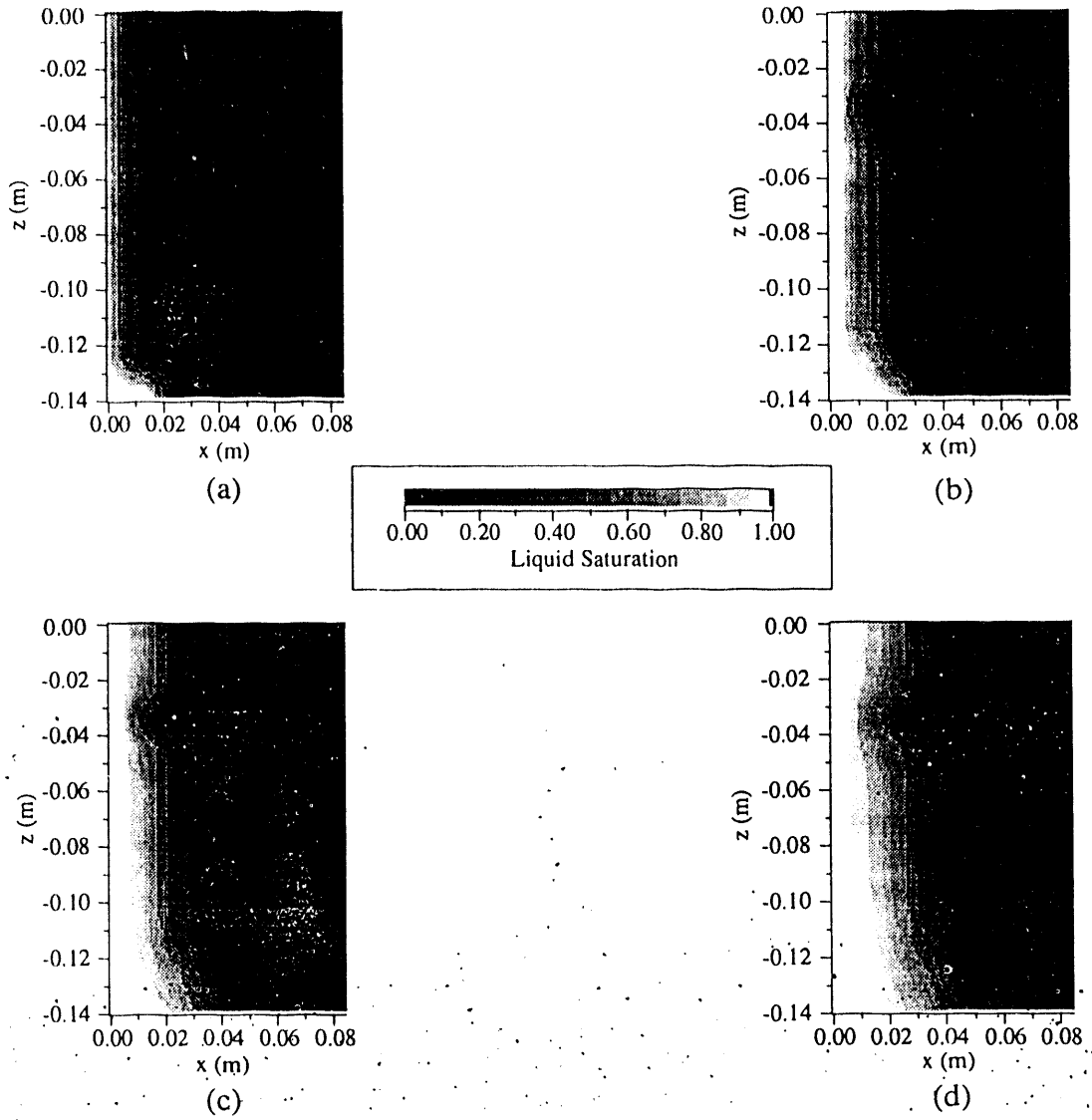

Figure 10. Numerical simulations of liquid saturations in the right-hand heterogeneous tuff matrix at a) 123 b) 957 c) 1890 and d) 3903 seconds using a linear capillary pressure function and a non-linear van Genuchten relative permeability function.

DATE
FILMED
6/30/94

END